Biochimica et Biophysica Acta, 548 (1979) 552—564
© Elsevier/North-Holland Biomedical Press

BBA 47775

THE ELECTRON SPIN RELAXATION OF THE ELECTRON ACCEPTORS OF PHOTOSYSTEM I REACTION CENTRE STUDIED BY MICROWAVE POWER SATURATION

HEINZ RUPP *, ANGEL DE LA TORRE ** and DAVID O. HALL

University of London, King's College, 68, Half Moon Lane, London, SE24 9JF (U.K.)

(Received February 26th, 1979)

Key words: ESR; Microwave power saturation; Photosystem I; Electron transfer; Iron-sulphur center; (Chloroplast)

Summary

Photosystem I particles from spinach were reduced by illumination at 77 K. Under these conditions the one-electron transfer from *P*-700 resulted in a reduction of only one acceptor molecule of the reaction centre. The EPR signals at $g = 2.05$, 1.94 and 1.86 were attributed to reduced centre A and the smaller signals at $g = 2.07$, 1.92 and 1.89 to reduced centre B. Reduction of both centres by dithionite in the dark lead to signals at $g = 2.05$, 1.99, 1.96, 1.94, 1.92 and 1.89. Thus, the features at $g = 2.07$ and 1.86 disappeared and new signals at $g = 1.99$ and 1.96 were observed. From the spectral changes it followed that the iron-sulphur centres A and B interact magnetically. Temperature dependent EPR spectra demonstrated a faster electron spin relaxation of centre A than of centre B.

These conclusions were corroborated using microwave power saturation of the respective EPR signals. The saturation data of the fully reduced centres A and B could not be fitted using the saturation equation for a one-electron spin system. The magnetic interaction between the [4Fe-4S] centres of the electron acceptors A and B resulted in saturation properties which are similar to those of the 2[4Fe-4S] ferredoxin from *Clostridium pasteurianum*.

For centre X a high proportion of homogeneous broadening of the EPR lines was inferred from the inhomogeneity parameter ($b = 1.83$). It was, therefore, concluded that centre X is most probably an anion radical of chlorophyll. From the low temperature necessary for observing the EPR signal of centre X

---

* Permanent address: Physiologisches Institut II der Universität Tübingen, Gmelinstrasse 5, 7400 Tübingen 1, F.R.G.

** Present address: University of California, Department of Cell Physiology, Berkeley, CA 94720, U.S.A.

Abbreviations: Hepes, *N*-2-hydroxyethylpiperazine-*N*'-2-ethanesulphonic acid; EPR, electron paramagnetic resonance.

followed that the drastic relaxation enhancement has to be attributed to a magnetic interaction of the anion radical with iron.

Introduction

In the primary photochemical reaction of Photosystem I of higher plants a charge separation occurs followed by rapid electron transfer [1]. The electron donor is *P*-700, a reaction centre chlorophyll [2]. The photoinduced changes related to *P*-700 can readily be monitored by optical [3] and electron paramagnetic resonance (EPR) [4] spectroscopy. By contrast, the identity of the electron acceptors proved to be less unequivocal. It was originally thought that a single membrane-bound ferredoxin may serve as a primary low-potential electron acceptor [5]. However, it soon became apparent that the EPR spectra could not be accounted for by only one membrane-bound ferredoxin. From potentiometric titrations it was concluded that at least three iron-sulphur centres were present [6]. Alternatively, it was proposed [7] that only two iron-sulphur centres, A and B, were necessary in order to explain the EPR properties — a magnetic interaction between centres A and B was assumed. Centre A and centre B are iron-sulphur centres of low oxidation-reduction mid-point potentials of —550 mV and —590 mV, respectively [6,7]. An even lower mid-point potential (approximately —730 mV) was found for a further electron accepting site, centre X [8]. It is widely thought that centre X can be regarded as a primary electron acceptor, whereas centres A and B are secondary acceptor molecules which function as electron traps [9—12]. The terms primary and secondary reflect the life-time of the states [13]. Furthermore, an acceptor molecule A_1 was postulated as intermediary acceptor between *P*-700 and centre X [14].

In an attempt to characterize further centre A, centre B and centre X, we studied their electron spin relaxation properties. Emphasis was placed on the magnetic interaction of centre A and B and on the structural properties of centre X. A convenient way for probing electron spin relaxation is by observing the EPR signal as a function of temperature and microwave magnetic field. In a study on a wide range of soluble iron-sulphur proteins it was found that the electron spin relaxation rate provides a useful criterion for characterizing the type of iron-sulphur centre and the presence of magnetic interactions with other paramagnetic systems [15].

Experimental

Materials

DE-23 DEAE-cellulose was from Whatman (Maidstone, U.K.); 2,5-dichlorophenolindophenol, Hepes, Tris and Triton X-100 (octylphenoxypolyethoxyethanol) were from Sigma (London) Chemical Co. (Kingston-upon-Thames, U.K.); L-ascorbate, methylviologen and sodium dithionite were from BDH Ltd. (Poole, Dorset, U.K.). All other chemicals were of the highest grade available commercially. Membranes for ultrafiltration (Diaflo XM 50) were from Amicon (High Wycombe, U.K.).

Photosystem I particles from spinach

Spinach (*Spinacia oleracia*) was obtained from Covent Garden market. Type E chloroplast fragments [16] were prepared as described by Whatley and Arnon [17]. Subchloroplast fragments enriched in Photosystem I reaction centre were prepared by the method of Vernon and Shaw [18] using the non-ionic detergent Triton X-100. After removal of the Photosystem II particles by centrifugation, Photosystem I particles were further purified by chromatography on a DEAE-cellulose column [19]. The fraction eluted by 0.3 M NaCl was concentrated by ultrafiltration on a Diaflo XM 50 membrane. The preparation used in the EPR experiments contained 0.3 M NaCl in 0.02 M Tris-HCl buffer, pH 8.0. Samples for experiments at high pH-value contained also 0.1 M glycine-NaOH buffer, pH 10.0. Chlorophylls *a* and *b* were determined by the procedure of Arnon [20] and *P*-700 was measured as described by Bengis and Nelson [21]. A chlorophyll concentration of 5—7 mg · ml^{-1} was used. The ratio of chlorophyll *a*/*b* in Photosystem I particles was 4.5. The molar ratio of *P*-700 to total chlorophyll was between 1 : 100 and 1 : 150. Photosystem I activity was assayed as oxygen uptake by using methyl viologen as electron acceptor and 2,5-dichlorophenolindophenol/ascorbate as electron donor [22]. The assay system contained in a final volume of 2 ml: 50 mM Hepes buffer (pH 7.6), 330 mM sorbitol, 5 mM $MgCl_2$, 2 mM $MnCl_2$, 2 mM EDTA, 5 mM NH_4Cl, 2 mM NaN_3, 0.2 mM methylviologen, 0.005 mM 3-(3,4-dichlorphenyl)-1,1-dimethylurea, 2 mM sodium ascorbate, 0.005 mM 2,5-dichlorophenolindophenol. The activity of Photosystem I particles following DEAE chromatography was 440 μequiv. electrons · mg^{-1} chlorophyll · h^{-1}.

EPR samples were prepared essentially as described by Evans et al. [12]. Illumination of the samples with white light was performed using a tungsten projector (1 kW) equipped with a heat filter.

EPR spectra

EPR spectra were recorded on a Varian E4 spectrometer (Varian Associates, Palo Alto, U.S.A.). Low temperature studies were performed using an ESR-9 continuous flow cryostat (Oxford Instruments, Oxford, U.K.). The temperature was measured by a gold/iron chromel thermocouple below the sample position and was calibrated with a carbon resistor thermometer. The carbon resistor was placed in a quartz EPR tube containing silicone oil. EPR spectra were recorded digitally on a Nicolet 1020A digital oscilloscope (Nicolet Instrument Corp., Madison, U.S.A.) interfaced to a HP 9830 calculator (Hewlett Packard Inc., Palo Alto, U.S.A.). As a check on the microwave power setting, EPR spectra of rubredoxin were recorded in a temperature range where the electron spin system was not saturated (see Fig. 1a of Ref. 15). By plotting $\log(S/\sqrt{P})$ vs. $\log P$, it was found that the experimental points followed a line parallel to the abscissa (S, signal amplitude; P, microwave power incident on the cavity). This indicates that the setting of the microwave power was correct in the range 0.5 to 200 mW. All spectra were recorded under standardized conditions (identical detector current, same quartz sample holder).

Microwave power saturation data

The experimental data of EPR signal size as a function of incident microwave power were fitted by a weighted least-squares procedure to the equation

$$S \propto \sqrt{P}/(1 + P/P_{1/2})^{b/2} \tag{1}$$

given by Beinert and Orme-Johnson [23], where b is the so-called inhomogeneity parameter and $P_{1/2}$ is the power for half-saturation with microwave energy. The inhomogeneity parameter reflects most probably the ratio of the Lorentzian spin packet width to the Gaussian envelope width. It provides a convenient means for characterizing the broadening mechanism of an EPR line. The curve fitting programme was devised by Dr. R. Cammack. The value for b could be specified or treated as free parameter. All EPR spectra observed in this study were free of rapid- and fast-passage effects. A detailed discussion on the theoretical aspects of microwave power saturation was given by Rupp et al. [15]. Calculations were carried out on a HP 9830 calculator and the saturation data were plotted on a Hewlett-Packard 7202A graphic plotter.

Results and Discussion

1. Changes of the EPR spectra dependent on temperature and microwave power

Photosystem I particles were incubated in quartz EPR tubes in the presence of 20 mM ascorbate at pH 8.0 (5 min, dark) and were frozen in liquid nitrogen in the dark. Illumination at 77 K resulted in a spectrum with strong lines at $g = 2.05$, 1.94 and 1.86 (Fig. 1). Additional features have been observed consistently [5,22,24,25] at approximately $g = 2.07$, 1.92 and 1.89. The free-radical signal I of P-700$^+$ indicates that these signals have been reduced by a photoreaction and are all linked to an electron-accepting site at the reaction centre. The EPR spectra of Fig. 1 are difference spectra (light minus dark) and thus, represent paramagnetic centres which became photoreduced in the frozen state at 77 K. Only functionally intact acceptor molecules are expected to become detectable under these conditions. As already noted, the temperature dependence of the signals provides a useful means for studying electron spin relaxation. In the temperature range 10—20 K the signals at $g = 2.05$, 1.94 and 1.86 predominate (Fig. 1a,b). The features near $g = 2.07$, 1.92 and 1.89 are detectable as shoulders. At higher temperatures the $g = 1.94$ resonance gradually disappears (Fig. 1c, d) and is hardly detectable at 38.1 K (Fig. 1e). A similar behaviour was found for $g = 2.05$ and $g = 1.86$. By contrast, the resonances at $g = 2.07$, 1.92 and 1.89 are more pronounced at higher temperatures (Fig. 1c, d). In addition to these signals a feature at $g = 2.09$ was detected. It can best be observed below approximately 15 K (Fig. 1a). A contribution from the Rieske iron-sulphur protein ($g = 2.02$, 1.90) [26] can be excluded.

Thus, from the temperature dependent EPR spectra three different types of signals can be distinguished: resonances (a) at $g = 2.07$, 1.92, 1.89, (b) at $g = 2.05$, 1.94, 1.86 and (c) at $g = 2.09$. We assign the $g = 2.05$, 1.94 and 1.86 features to centre A and the $g = 2.07$, 1.92 and 1.89 features to centre B. Since the signals following illumination at 77 K were increased by a factor of 9, the probability is low that in a particular reaction centre both centres A and B are reduced. (Note, photoreduction by illumination at 77 K results in the transfer of only one electron from P-700.) The composite spectrum arises, therefore,

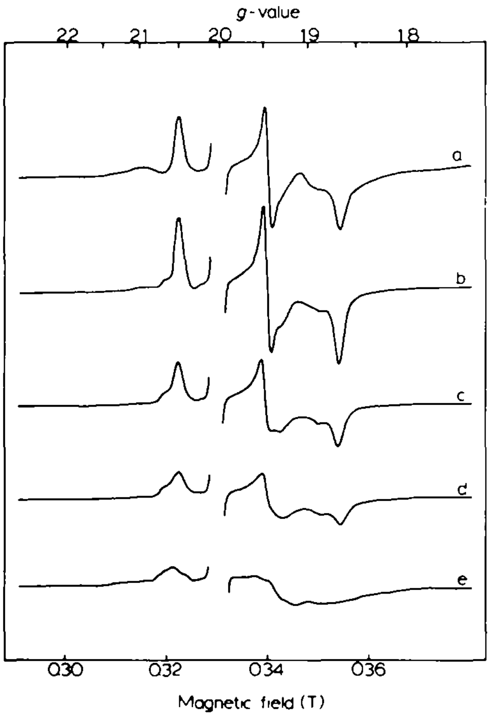

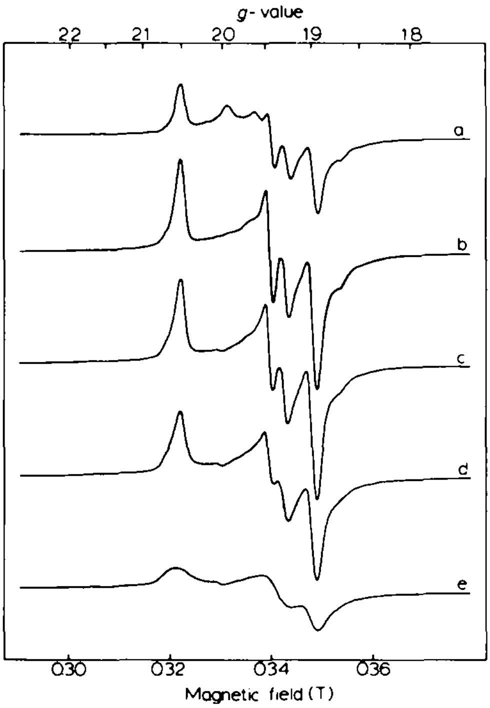

Fig. 1. Temperature dependence of the light-induced EPR signals of Photosystem I particles. Spectra were recorded of particles kept in the dark (5 min) in the presence of 20 mM ascorbate (pH 8.0), then spectra were recorded following illumination (77 K, 1 min). The light-induced spectra were obtained as light minus dark difference spectra using a Nicolet 1020A digital oscilloscope; (a) 10.4 K, (b) 18.3 K, (c) 25.4 K, (d) 28.8 K, (e) 38.1 K; microwave power 10 mW; modulation amplitude 1 mT; microwave frequency 9.25 GHz; the receiver gain of spectrum (e) was 2.5 times greater than that of the other spectra.

Fig. 2. Temperature dependence of the EPR signals of Photosystem I particles reduced by 10 mM dithionite in the dark (pH 10.0, 40 min); (a) 10.4 K, (b) 18.3 K, (c) 25.4 K, (d) 28.8 K, (e) 38.1 K; microwave power 10 mW; modulation amplitude 1 mT; microwave frequency 9.25 GHz.

from reaction centres which contain either reduced centre A or to a much lesser extent reduced centre B. Under thermodynamically controlled conditions, a one-electron transfer would not result in a reduction of centre X or the intermediary acceptor A_1 [27]. However, in the frozen state at 77 K the electron transfer would depend also on the mechanisms of electron tunneling. Obviously, under these conditions a reduction of electron acceptors having more negative potentials than centres A and B might still be possible. Although at present we have no strong evidence that the $g = 2.09$ signal is related to Photosystem I, we are inclined to relate this resonance with an intermediary electron acceptor, probably between *P*-700 and centre X.

Further reduction of the electron acceptors was achieved by incubation of Photosystem I particles at pH 10.0 with 10 mM dithionite for 40 min in the dark. Pronounced signals were observed at $g = 2.05, 1.99, 1.96, 1.94, 1.92, 1.89$ and a small feature at 1.86. Signals characteristic of centre X were not detected. This indicates that the secondary electron acceptors were not fully reduced (Fig. 2a). However, in most reaction centre particles both centres A and B are reduced and are in the paramagnetic state. In contrast to the spectra of isolated centres A and B, only small signals were observed at $g = 2.07$ and 1.86. Signals which were not detected for the isolated centres (Fig. 1) occur at $g = 1.99$ and $g = 1.96$ (Fig. 2a) [28]. The latter features are hardly detectable above 20 K. The $g = 1.96$ component was observed previously using potentiometric titrations [6] — it was not seen at an oxidation-reduction potential of −562 mV, but was seen at −612 mV. Thus, also the $g = 1.99$ and 1.96 signals are not related to Rieske's iron-sulphur protein which has an oxidation-reduction mid-point potential of +290 mV [26]. The $g = 1.94$ and 1.86 resonances vanish above approximately 30 K (Fig. 2d, e) as in Fig. 1. Thus, the spectra of Fig. 1e and Fig. 2e are strikingly similar. The $g = 1.94$ and 1.86 signals broaden out at lower temperatures than the $g = 1.92$ and 1.89 signals. This indicates a faster electron spin relaxation for iron-sulphur centre A. It is noteworthy that this difference in relaxation properties is maintained despite the presence of two paramagnetic centres in the Photosystem I reaction centre.

A way for partially reducing the iron-sulphur centres is by oxidation-reduction potential titration in the presence of mediators [6,7]. A serious drawback arising from the presence of oxidation-reduction mediators is a large free-radical signal which interferes with signals of Photosystem I. Furthermore, mediators in a paramagnetic form might interact with the electron carriers thus altering their relaxation behaviour. These complications can be avoided by reducing the electron acceptors by dithionite using different reaction times. Representative spectra are shown in Fig. 3b—e. Following reduction with 10 mM dithionite for 2 min in the dark, the EPR signals (Fig. 3b) are similar to those observed for particles kept dark and then illuminated at 77 K (Fig. 3a). Longer reduction times (10 min, Fig. 3c; 20 min, Fig. 3d) result in progressive reduction of both centres A and B. The $g = 1.86$ feature disappears and in parallel signals at $g = 1.99$, 1.96 and 1.89 appear. The $g = 1.99$ and 1.96 signals are best seen at high microwave power, where P-700$^+$ is strongly saturated. It should be pointed out that the $g = 1.99$ signal might be obscured by the trough of the free-radical signal of P-700$^+$. It would be not justified in this case to use the peak to peak height of the free-radical as a measure for P-700$^+$. Following reduction for 35 min, the $g = 1.99$ and 1.96 signals are further increased, whereas the $g = 1.86$ feature has become very small (Fig. 3e).

It is noteworthy that the $g = 1.99$ and 1.96 signals can be observed although centre X is oxidized (Fig. 3e). From the appearance of new signals in parallel to the reduction of both centres A and B in a reaction centre we conclude that the centres interact magnetically. Depending on the type of interaction (dipolar or exchange interaction) and the distance between the centres, a splitting or shift of EPR lines and a change in the electron spin relaxation properties is expected. Spectral changes are observed for both centres upon interaction. The $g = 2.07$ signal of centre B vanishes and also the $g = 1.86$ signal of centre A. It is not feasible to assign different features of the interaction-type spectrum to a particular centre. Shifts of resonances due to interaction with other paramagnetic centres are well established. For the eight-iron bacterial ferredoxins a low-field resonance is shifted to higher magnetic field upon reduction of the second iron-sulphur centre [15,29,30] and for the Rieske's iron-sulphur

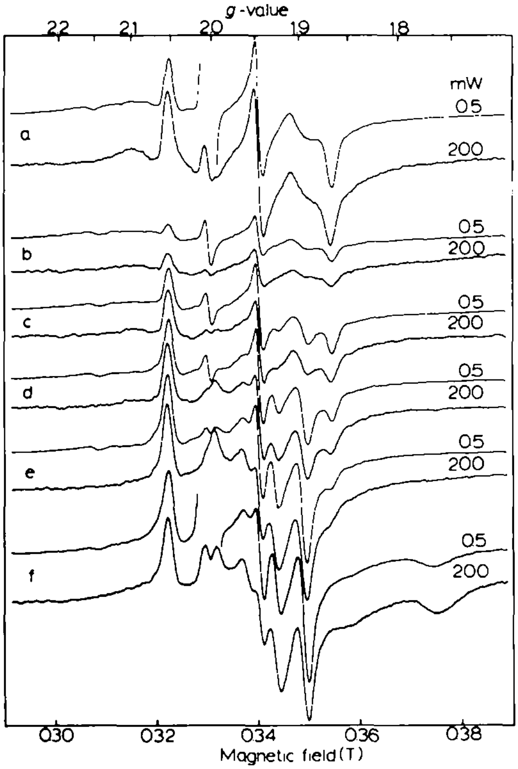

Fig. 3. EPR signals of Photosystem I particles reduced in the dark by 10 mM dithionite (pH 10.0) for (b) 2 min, (c) 10 min, (d) 20 min, (e) 35 min. Spectra were recorded with 0.5 mW and 200 mW microwave power. For comparison are shown spectra also of (a) illuminated particles (77 K, 1 min) after being kept in the dark for 5 min (20 mM ascorbate, pH 8.0) and (f) of particles which were illuminated in the presence of 10 mM dithionite (pH 10.0) for 2 min and were illuminated during freezing in liquid nitrogen. All spectra were recorded at 10.4 K; modulation amplitude 1 mT; microwave frequency 9.25 GHz; receiver gain 500 (for 0.5 mW microwave power) and 100 (for 200 mW microwave power).

protein in mitochondria the high-field line is also shifted to higher field due to interaction with cytochrome *b*-562 [31].

The primary electron acceptor was reduced by illumination of Photosystem I particles in the presence of 10 mM dithionite followed by illumination during freezing in liquid nitrogen (Fig. 3f). As already noted, the $g = 1.99$ resonance cannot be observed in the presence of a large *P*-700$^+$ signal at low microwave power, but becomes detectable at high microwave power (Fig. 3f). It follows that centre X does not induce any further line splitting of the interaction-type spectrum of centres A and B. However, this does not imply a distance greater than 1.0 nm between centre X and centres A and B.

2. *Simulation of microwave power saturation curves*

For the EPR spectra reported in Fig. 1 and Fig. 2 a microwave power of 10 mW was used. In order to characterize further the electron spin systems contributing to the complex spectra, spectra were recorded with microwave power ranging from 0.5 mW to 200 mW. The saturation data are presented in a

$\log(S/\sqrt{P})$ against $\log P$ plot, where S is the signal amplitude and P is the microwave power incident on the cavity. In this presentation, a line parallel to the abscissa indicates that there is no saturation. Increasing saturation results in a downward slope. A graphical method has been described for obtaining the microwave powers for half-saturation [23]. Alternatively, the experimental saturation data can be fitted by a weighted least-squares procedure to equations for homogeneously and inhomogeneously broadened lines [15]. In Eqn. 1 ($S \propto \sqrt{P}/(1 + P/P_{1/2})^{b/2}$), b is the inhomogeneity parameter which depends on the broadening mechanism. It is equal to 4.0 for a homogeneously and equal to 1.0 for an inhomogeneously broadened line [15]. Theoretical microwave power saturation curves ($b = 1.22$) for different $P_{1/2}$ values were reported [32].

A deviation from theoretical saturation behaviour calculated for a one-electron spin system is expected for cases where two or more components of different relaxation behaviour contribute to the EPR properties and where the individual signals overlap. The extent of deviation depends on the difference between the $P_{1/2}$ values and on the ratio of the individual components contributing to the overlapped signal. To illustrate this point, saturation data were calculated using Eqn. 1 and an inhomogeneity parameter of 1.0 (inhomogeneously broadened line). It was assumed that two components A and B of different $P_{1/2}$ values overlap in a varying ratio. In Fig. 4C theoretical saturation data are given for a component A ($P_{1/2} = 1$ mW) (Fig. 4Ce) and a component B ($P_{1/2} = 10$ mW) (Fig. 4Ca). In addition, saturation data are shown for overlapped signals, i.e components A and B are mixed in the ratio 0.75 A : 0.25 B (Fig. 4Cd), 0.5 A : 0.5 B (Fig. 4Cc) and 0.25 A : 0.75 B (Fig. 4Cb). In all cases the saturation points were fitted by the weighted least-squares procedure to the saturation Eqn. 1 for a one-electron spin system, $P_{1/2}$ was treated as a free parameter. It is noteworthy that the data points apparently can be fitted, if the ratio of $P_{1/2}(B)/P_{1/2}(A)$ is smaller than approximately 10 (Fig. 4C). At a ratio of 100 (Fig. 4B) or 1000 (Fig. 4A) a deviation becomes apparent. An interesting feature of the last two cases is that a small contribution (25%) of a fast relaxing component to a slow relaxing one results in a pronounced deviation (Fig. 4Bd). By contrast, a similar contribution of a slow relaxing species to a fast relaxing one is less obvious (Fig. 4Bb).

It was found previously that the saturation data of proteins containing only one iron-sulphur centre can all be fitted using theoretical saturation curves [15]. The microwave powers for half-saturation were markedly different for [2Fe-2S] and [4Fe-4S] centres, thus, providing a diagnostic tool for distinguishing the centres. Magnetic interactions with other paramagnetic species must be absent for this analysis. It should be noted that different EPR lines of the same iron-sulphur cluster can exhibit slightly different saturation behaviour. Thus, for spinach ferredoxin the half-saturation powers were 0.48 mW ($g_z = 2.05$), 1.14 mW ($g_y = 1.96$) and 1.59 mW ($g_x = 1.89$) at 14.7 K. The inhomogeneity parameter b was 1.34 for all features. However, there was still a marked difference in the saturation properties of [2Fe-2S] and [4Fe-4S] centres.

3. *Microwave power saturation of the secondary electron acceptors*

From the temperature dependence of the EPR properties it follows that the

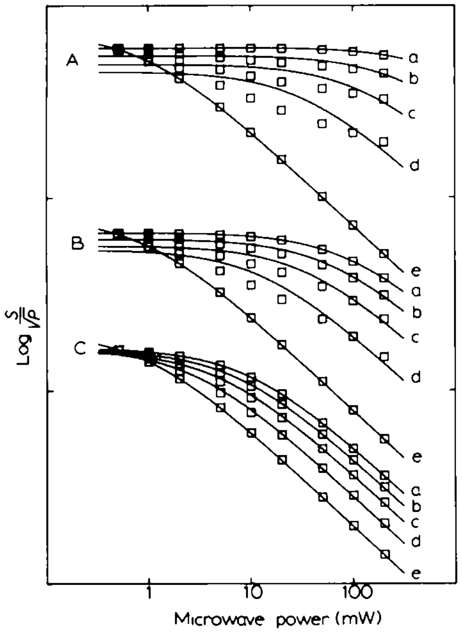

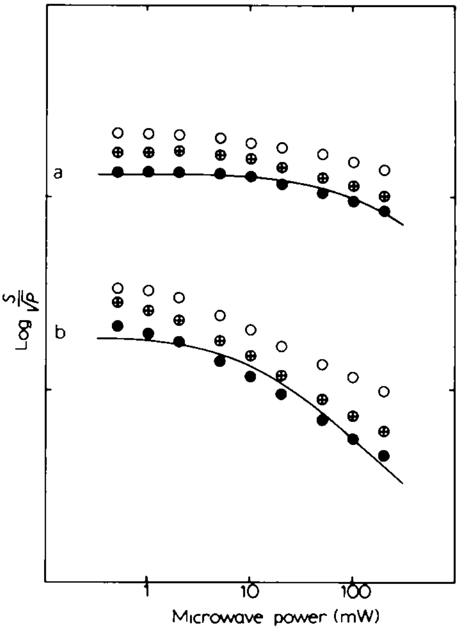

Fig. 4. Theoretical power saturation data for two components A and B which overlap in a varying ratio. The contribution to the saturation data of each of the species was varied in the following way: (a) 100% B, no A; (b) 75% B, 25% A; (c) 50% B, 50% A; (d) 25% B, 75% A; (e) no B, 100% A. The half-saturation power $P_{1/2}$ of component A was kept constant ($P_{1/2} = 1$ mW) throughout, whereas $P_{1/2}$ for component B was changed from (Fig. 4C) 10 mW to (Fig. 4B) 100 mW and to (Fig. 4A) 1000 mW. The saturation points were calculated using Eqn. 1 for an inhomogeneously broadened line ($b = 1.0$). The data points were then fitted using a weighted least squares procedure by treating $P_{1/2}$ as free parameter assuming a one-electron spin system.

Fig. 5. Microwave power saturation data of Photosystem I particles which were illuminated at 77 K (1 min) after being kept dark for 5 min in the presence of 20 mM ascorbate (pH 8.0); (a) 21.8 K, (b) 14.2 K. The signal amplitude of the (○) $g = 2.05$, (⊕) $g = 1.86$ and the (●) $g = 1.94$ features was used. The data points of the $g = 1.94$ signal were fitted by treating $P_{1/2}$ as free parameter ($b = 1.0$). A higher inhomogeneity parameter did not result in a better fit.

signals at $g = 1.94$ and 1.86 are not linked to the same site as the signals at $g = 1.92$ and 1.89. This is in agreement with oxidation-reduction potential titrations [7]. Microwave power saturation curves for Photosystem I particles kept in the dark and illuminated at 77 K further substantiate this conclusion. Both the $g = 1.94$ and 1.86 resonances show similar saturation behaviour (Fig. 5). An intriguing feature is the small deviation of the data points from theoretical saturation curves which becomes particularly obvious at low temperature (14.2 K) (Fig. 5b). The $g = 2.05$ resonance exhibits the greatest deviation from theoretical saturation behaviour of a one-electron spin system. This suggests contributions arising from species of different relaxation behaviour. As demonstration in Fig. 4 a deviation from theoretical saturation behaviour of a one-electron spin system will be apparent when two species of different saturation behaviour contribute to a particular signal. As already pointed out, centres A and B have different electron spin relaxation rates. Moreover, the signals of the isolated centres overlap to a great extent. A deviation from the saturation characteristics as calculated for one species is, therefore, expected.

In Fig. 6 are given the saturation data of all EPR features of the electron acceptors of Photosystem I beside centre X. It is apparent that they cannot be fitted using Eqn. 1 for a one-electron spin system. Although the analysis becomes then less straightforward, it is still possible to detect changes in the saturation characteristics. In Fig. 6b, e the saturation data are compared for Photosystem I particles reduced by dithionite for (▲) 5 min and (■) 35 min. Following reduction for 5 min it is expected that predominantly isolated centres A and B are present, whereas after 35 min mostly interacting centres are expected. In the latter case, the signals exhibit a stronger deviation from theoretical saturation behaviour as calculated for a one-electron spin system. These changes in the saturation properties clearly support the concept that centres A and B do interact.

Well characterized examples for a spin coupling between iron-sulphur centres are the 2[4Fe-4S] ferredoxins from *C. pasteurianum* and *Micrococcus lactilyticus* [33,34]. For *C. pasteurianum* ferredoxin the saturation data could also not be fitted using theoretical curves for a one-electron spin system [15]. The analogy of the saturation behaviour of the Fe-S centres A and B to *C. pasteurianum* ferredoxin is striking. Since it has been found that both centres A and B are [4Fe-4S] centres [19], this might indicate a similar type of interaction between centres A and B as in *C. pasteurianum* ferredoxin.

In this respect it is worthwhile to consider some of the implications involved in an interaction between centres A and B. Firstly, the quantitative determination of centre B in the presence of reduced centre A by double integration of the interaction-type EPR spectrum becomes rather ambiguous [35]. Recent examples are studies [36] on the stoichiometry of centres of S-1 and S-2 of the mitochondrial succinate dehydrogenase. S-1 can be observed by itself after reduction with succinate, whereas S-2 can be seen only under conditions when both centres are reduced. Since the centres are interacting [36—38], it is not any more permissible to quantify S-2 by subtracting the signal of S-1 from that of S-1 plus S-2 [36]. A mechanism which involves only a decrease of the spectral amplitude, but no significant line broadening was described by Leigh [39]. Secondly, from the existence of such an interaction between centres A and B a small distance (less than about 1 nm) between the iron-sulphur centres has to be inferred.

4. *Microwave power saturation of the primary electron acceptor*

At present, the chemical nature of the primary electron acceptor X is unknown. Using ^{57}Fe enriched membrane fractions from *Chlorogloea fritschii* a line broadening due to unresolved hyperfine splitting was detected for centre A and centre B as was expected for iron-sulphur centres. However, no significant increase in the linewidth was observed for the $g = 1.76$ signal of centre X [40]. A way of probing the structure of centre X is by comparing its saturation characteristics with those of well-defined iron-sulphur proteins. Although the factors contributing to the inhomogeneity parameter b are not fully understood at present, it proved of considerable diagnostic value. The saturation data of [2Fe-2S] proteins could be fitted best using $b = 1.34$ and of [4Fe-4S] proteins using $b = 1.22$. For the 1Fe centre of rubredoxin an inhomo-

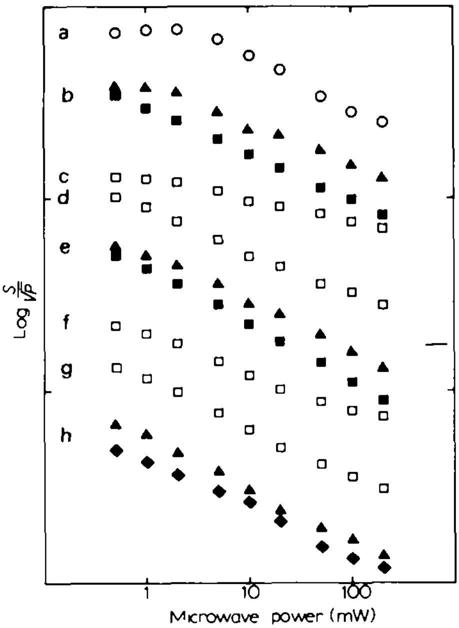

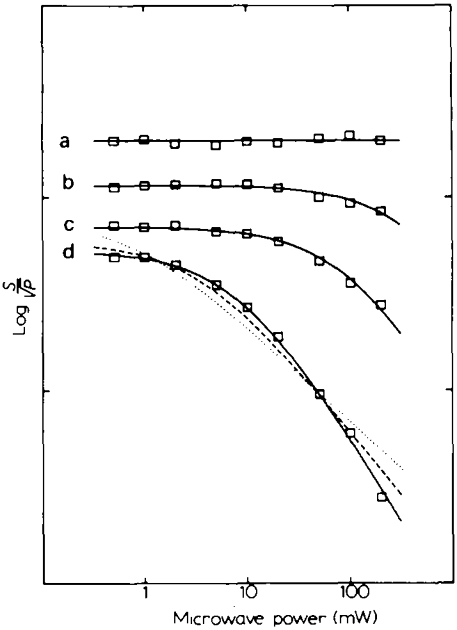

Fig. 6. Microwave power saturation data of different spectral features of Photosystem I particles; (a) $g = 2.09$, (b) $g = 2.05$, (c) $g = 1.99$, (d) $g = 1.96$, (e) $g = 1.94$, (f) $g = 1.92$, (g) $g = 1.89$, (h) $g = 1.86$. The symbols represent different samples: (○) illuminated Photosystem I particles (77 K, 1 min) after being kept in the dark (5 min, 20 mM ascorbate, pH 8.0); Photosystem I particles reduced by 10 mM dithionite (pH 10.0) in the dark and frozen after (△) 5 min, (◇) 20 min and (□) 35 min. The filled-in symbols represent same spectral features which are compared for two different samples. All spectra were recorded at 10.4 K; modulation amplitude 1 mT; microwave frequency 9.25 GHz.

Fig. 7. Microwave power saturation data for the $g = 1.76$ feature of centre X at (a) 11.7 K, (b) 10.7 K, (c) 9.7 K and (d) 8.3 K. Photosystem I particles were illuminated in the presence of 10 mM dithionite (pH 10.0) for 2 min and illuminated during freezing. The data points were fitted using a weighted least squares procedure assuming $b = 1.83$ and treating $P_{1/2}$ as free parameter. The inhomogeneity parameter $b = 1.83$ was obtained for the saturation data at 8.3 K by treating b and $P_{1/2}$ as free parameters. For the data at 8.3 K are also given saturation curves which based on (· · · · · ·) $b = 1.0$ and (- - - - - -) $b = 1.34$, $P_{1/2}$ was treated as free parameter; modulation amplitude 1 mT; microwave frequency 9.25 GHz.

geneity parameter of 1.63 was found [15]. This shows that the ratio of the width of the spectral envelope to the width of the spin packet increased from rubredoxin to [2Fe-2S] ferredoxins to [4Fe-4S] ferredoxins.

In Fig. 7 the saturation curves are given for the $g = 1.76$ signal of centre X at different temperatures. A striking feature of the saturation data is the high proportion of homogeneous broadening of the line. Using the weighted least squares procedure to Eqn. 1 and treating $P_{1/2}$ and the inhomogeneity parameter as free parameters, $b = 1.83$ gave the best fit all over the temperature range studied. For comparison, theoretical curves are shown assuming $b = 1.0$ (Fig. 7d, dotted line) and $b = 1.34$ (Fig. 7d, broken line) and treating $P_{1/2}$ as a free parameter. It is obvious that centre X cannot be treated like a [4Fe-4S] ($b = 1.22$) or [2Fe-2S] ($b = 1.34$) protein. It might be argued that membrane-bound iron-sulphur centres have a drastically altered broadening mechanism. However, this is not the case, as microwave power saturation studies of iron-sulphur centres of the mitochondrial membrane have shown [38,41]. We have to conclude that centre X is not a typical [2Fe-2S] or [4Fe-4S] centre.

The high degree of homogeneous line broadening can best be explained by assuming a radical structure for centre X. A prime candidate would be the anion of chlorophyll [42]. However, the chlorophyll anion radical in dimethylformamide exhibits featureless EPR signals and is strongly saturated at cryogenic temperatures [42]. In order to account for the distinct properties of centre X, we have to conclude that a fast relaxing ion, most probably iron, interacts with the anion radical. This would explain the high relaxation rate of centre X, as seen from the low temperature necessary for observing its EPR signal (below approximately 12 K). Furthermore, the anisotropic spectrum ($g_x = 2.06$, $g_y = 1.86$, $g_z = 1.76$) could be rationalized by a magnetic coupling with iron. An interaction of the chlorophyll anion with the iron-sulphur centres (Ref. 38 in Fujita et al. [42]) of the secondary electron acceptors A and B is not expected to lead to the high relaxation rate of centre X. Only a metal iron would be in a position to provide such a strong relaxation enhancement for the anion radical. (Note, both [4Fe-4S] centres of the electron acceptors A and B are more saturated than centre X.)

In the bacterial photosystem a quinone-iron complex is involved in the traditional primary electron acceptor [13,43—45]. Thus, it would be of great interest to compare centre X of plant chloroplasts with the primary electron acceptor of the bacterial photosystem with regard to their saturation properties. This would be a promising way of detecting any structural relationship between the well characterized quinone-iron complex of photosynthetic bacteria and the anonymously called acceptor X of plant chloroplasts. It is attractive to assume that in the primary electron acceptor of bacteria and of plants the basic structure, i.e. iron interacting with a radical, is maintained. However, for bacteria a quinone and for plants a chlorophyll would serve as the acceptor molecules. This might explain the large difference in the oxidation-reduction potentials (—730 mV for green plants and about —200 mV for bacteria).

Acknowledgements

H.R. was a recipient of a fellowship (No. 245/1) of the Deutsche Forschungsgemeinschaft and A.T. was a recipient of a scholarship of the Spanish Ministry of Science. This study was supported by the NATO Research Programme (No. 1256) and the U.K. Science Research Council. The expert help of Mrs. K. Rupp and Dr. P. Morris is greatly appreciated. We are indebted to Dr. M.C.W. Evans, University College London for the use of the Nicolet oscilloscope and to Dr. R. Cammack for the computing facilities and for communicating unpublished data on *Phormidium* Photosystem I. We also wish to express our gratitude to Dr. J.R. Bolton, University of Western Ontario, London, Canada for his valuable criticism of the manuscript.

References

1 Bolton, J.R. (1977) in Primary Processes of Photosynthesis (Barber, J., ed.), pp. 188—202, Elsevier, Amsterdam

2 Bolton, J.R. and Warden, J.T. (1976) Ann. Rev. Plant Physiol. 27, 375—383
3 Kok, B. (1956) Biochim. Biophys. Acta 22, 399—401
4 Evans, M.C.W., Sihra, C.K. and Slabas, A.R. (1977) Biochem. J. 162, 75—85
5 Malkin, R. and Bearden, A.J. (1971) Proc. Natl. Acad. Sci. U.S.A. 68, 16—19
6 Ke, B., Hansen, R.E. and Beinert, H. (1973) Proc. Natl. Acad. Sci. U.S.A. 70, 2941—2945
7 Evans, M.C.W., Reeves, S.G. and Cammack, R. (1974) FEBS Lett. 49, 111—114
8 Ke, B., Dolan, E., Sugahara, K., Hawkridge, F.M., Demeter, S. and Shaw, E.R. (1977) Photosynthetic Organelles, Special Issue of Plant Cell Physiol., pp. 187—199
9 McIntosh, A.R., Chu, M. and Bolton, J.R. (1975) Biochim. Biophys. Acta 376, 308—314
10 Evans, M.C.W., Sihra, C.K., Bolton, J.R. and Cammack, R. (1975) Nature 256, 668—670
11 McIntosh, A.R. and Bolton, J.R. (1976) Biochim. Biophys. Acta 430, 555—559
12 Evans, M.C.W., Sihra, C.K. and Cammack, R. (1976) Biochem. J. 158, 71—77
13 Okamura, M.Y., Issacson, R.A. and Feher, G. (1975) Proc. Natl. Acad. Sci. U.S.A. 72, 3491—3495
14 Dismukes, G.C., McGuire, A., Blankenship, R. and Sauer, K. (1978) Biophys. J. 21, 239—256
15 Rupp, H., Rao, K.K., Hall, D.O. and Cammack, R. (1978) Biochim. Biophys. Acta 537, 255—269
16 Hall, D.O. (1972) Nature 235, 125—126
17 Whatley, F.R. and Arnon, D.I. (1963) in Methods in Enzymology (Colowick, S.P. and Kaplan, N.O., eds.), Vol. 6, pp. 308—313, Academic Press, New York
18 Vernon, L.P. and Shaw, E.R. (1971) Methods Enzymol. 23A, 277—289
19 Cammack, R. and Evans, M.C.W. (1975) Biochem. Biophys. Res. Commun. 67, 544—549
20 Arnon, D.I. (1949) Plant Physiol. 24, 1—15
21 Bengis, C. and Nelson, N. (1975) J. Biol. Chem. 250, 2783—2788
22 Evans, M.C.W., Telfer, A. and Lord, A.V. (1972) Biochim. Biophys. Acta 267, 530—537
23 Beinert, H. and Orme-Johnson, W.H. (1967) in Magnetic Resonance in Biological Systems (Ehrenberg, A., Malmström, B.G. and Vänngård, T., eds.), pp. 221—247, Pergamon Press, Oxford
24 Bearden, A.J. and Malkin, R. (1976) Biochim. Biophys. Acta 430, 538—547
25 Williams-Smith, D.L., Heathcote, P., Sihra, C.K. and Evans, M.C.W. (1978) Biochem. J. 170, 365—371
26 Malkin, R. and Aparicio, P.J. (1975) Biochem. Biophys. Res. Commun. 63, 1157—1160
27 Sauer, K., Mathis, P., Acker, S. and Van Best, J.A. (1978) Biochim. Biophys. Acta 503, 120—134
28 Dismukes, G.C. and Sauer, K. (1978) Biochim. Biophys. Acta 504, 431—445
29 Zubieta, J.A., Mason, R. and Postgate, J.R. (1973) Biochem. J. 133, 851—854
30 Orme-Johnson, W.H. and Beinert, H. (1969) Biochem. Biophys. Res. Commun. 36, 337—344
31 Beinert, H. (1977) in Iron-Sulfur Proteins (Lovenberg, W., ed.), Vol. 3, pp. 61—100, Academic Press, New York
32 Rupp, H., Rao, K.K., Hall, D.O. and Moore, A.L. (1978) in Plant Mitochondria (Ducet, G. and Lance, C., eds.), pp. 93—100, Elsevier, Amsterdam
33 Gersonde, K., Schlaak, H.-E., Breitenbach, M., Parak, F., Eicher, H., Zgorzalla. W., Kalvius, M.G. and Mayer, A. (1974) Eur. J. Biochem. 43, 307—317
34 Mathews, R., Charlton, S., Sands, R.H. and Palmer, G. (1974) J. Biol. Chem. 249, 4326—4328
35 Heathcote, P., Williams-Smith, D.L., Sihra, C.K. and Evans, M.C.W. (1978) Biochim. Biophys. Acta 503, 333—342
36 Beinert, H., Ackerell, B.A.C., Vinogradov, A.D., Kearney, E.B. and Singer, T.P. (1977) Arch. Biochem. Biophys. 182, 95—106
37 Ohnishi, T., Salerno, J.C., Winter, D.B., Lim, J., Yu, C.A., Yu, L. and King. T.E. (1976) J. Biol. Chem. 251, 2094—2104
38 Rupp, H. and Moore, A.L. (1979) Biochim. Biophys. Acta 548, 16—29
39 Leigh, J.S. (1970) J. Chem. Phys. 52, 2608—2612
40 Evans, E.H., Cammack, R. and Evans, M.C.W. (1976) Biochem. Biophys. Res. Commun. 68, 1212—1218
41 Moore, A.L. and Rupp, H. (1978) FEBS Lett. 93, 73—77
42 Fujita, I., Davis, M.S. and Fajer, J. (1978) J. Am. Chem. Soc. 100, 6280—6282
43 Prince, R.C., Tiede, D.M., Thornber, J.P. and Dutton, P.L. (1977) Biochim. Biophys. Acta 462, 467—490
44 Prince, R.C. (1978) Biochim. Biophys. Acta 501, 195—207
45 Prince, R.C., Dutton, P.L., Clayton, B.J. and Clayton, R.K. (1978) Biochim. Biophys. Acta 502, 354—358